Soils and Rocks
An International Journal of Geotechnical and Geoenvironmental Engineering
www.soilsandrocks.com
ISSN 1980-9743
ISSN-e 2675-5475

Textured high-density polyethylene geomembranes in geotechnical and environmental engineering: an overview

Maria Alejandra Aparicio-Ardila[1#], Jefferson Lins da Silva[1]

Review Article

Keywords
Geosynthetics
HDPE geomembranes
Textured geomembranes
Sanitary landfills
Geosynthetics in mining

Abstract

Textured high-density polyethylene (HDPE) geomembranes are widely used as liners in environmental containment systems, particularly in mining facilities and sanitary landfills. Their textured surfaces enhance interface friction, improving the mechanical stability of geosynthetic barrier systems. This article presents a comprehensive review of their applications, interface behavior, and long-term performance, with emphasis on durability. Key manufacturing processes and technological advances, including conductive, Ethylene Vinyl Alcohol (EVOH), and colored layers, are discussed. Beyond manufacturing aspects, installation quality is also addressed, emphasizing that proper welding procedures, certified installers, and field quality control are essential to ensure long-term performance and minimize premature failures. Although various texturing methods are employed, the literature still lacks systematic comparative studies that isolate variables such as asperity height, which limits understanding of how manufacturing processes influence interface behavior. Furthermore, recent findings suggest that surface texturing, depending on material formulation and exposure conditions, may accelerate antioxidant depletion, potentially affecting service life. Field exposure and exhumation studies remain scarce, yet they are fundamental for validating laboratory predictions and refining design approaches. The findings highlight the need for standardized testing protocols and long-term studies tailored to the environmental conditions under which textured HDPE geomembranes are exposed. Overall, the information presented herein provides both scientific insight and practical guidance for the selection of materials and installation practices that ensure the long-term durability of geotechnical and environmental barrier systems.

1. Introduction

Polyethylene (PE) geomembranes, particularly HDPE geomembranes with density ≥ 0.941 g/cm^3, are widely used as hydraulic barriers due to their high chemical resistance, ease of installation, and cost-effectiveness. A variety of PE geomembranes are available, manufactured using different resins and additives. As a result, service life can vary significantly depending on exposure conditions, chemical environment, and temperature, ranging from decades to millennia (Clinton & Rowe, 2024; Rowe & Fan, 2024).

In waste containment systems, HDPE geomembranes significantly reduce the need for natural soil, minimizing environmental impacts from soil extraction and transport (Palmeira, 2025). HDPE geomembranes may be smooth or textured. Textured geomembranes are recommended in environmentally sensitive applications such as landfill liners and mining facilities due to their enhanced interface friction, which improves stability and reduces slippage (Costa Junior et al., 2023). Their primary function is to increase interface friction angles. These geomembranes are produced in various thicknesses depending on the application, typically 1.5 mm for mining (e.g., Rowe & Ewais, 2015) and 2.0 mm for Municipal Solid Waste (MSW) landfills (e.g., Jucá et al., 2021), and may be textured on one or both sides. Improved frictional properties also allow steeper slopes (Müller, 2007).

Beyond landfills and mining, textured HDPE geomembranes have been applied in other geotechnical and environmental works. For example, at the Salto and São Salvador hydroelectric power plants in Brazil, double-sided textured 1.5 mm HDPE geomembranes were used as upstream impermeable blankets to minimize preferential flow paths that could occur with smooth-surface geomembranes (Cardoso et al., 2010; Pierozan et al., 2019). In Thailand, Soralump et al. (2021) reported the use of textured geomembranes with a Geosynthetic Clay Liner (GCL) on

#Corresponding author. E-mail address: maparicio@usp.br
[1]Universidade de São Paulo, Escola de Engenharia de São Carlos, Departamento de Geotecnia, São Carlos, SP, Brasil.

Submitted on July 31, 2025; Final Acceptance on December 15, 2025; Discussion open until August 31, 2026.
Editor: Renato P. Cunha
https://doi.org/10.28927/SR.2026.012325

the downstream slope of the Lam Ta Khong dam, observing reduced settlement. Another application is vertical barriers to confine contaminated soil and prevent lateral migration of contaminants (Palmeira, 2025).

For successful performance, geomembrane lining systems must ensure interface stability and containment. The shear strength between geosynthetics and surrounding materials is critical. In landfill applications, adequate friction between the geomembrane and adjacent layers prevents interface failure and maintains containment integrity (Gardoni et al., 2025). However, achieving complete impermeability remains a challenge, as zero leakage is unrealistic and leakage may result from improper installation or material degradation (Giroud, 2016).

Despite their widespread use, the literature still presents gaps in understanding the behavior and performance of textured HDPE geomembranes (Lavoie et al., 2020). Therefore, this study provides an overview of textured HDPE geomembranes in geotechnical and environmental engineering, including manufacturing methods, technologies, interface behavior, degradation mechanisms, installation procedures, and recent durability findings.

2. Manufacturing methods

2.1 Texturing processes

All polyolefin geomembranes, including HDPE, Linear Low-Density Polyethylene (LLDPE), and flexible Polypropylene (PP), are manufactured by extrusion, either as single-layer films or by coextrusion. Typical HDPE formulations contain 95-98% polymer resin, 2-3% carbon black, and 0.25-1% antioxidants and stabilizers. Although additive packages are proprietary, they generally combine phosphites, hindered phenols, thiosynergists or hindered amines, and Hindered Amine Light Stabilizers (HALS) to protect against thermal-oxidative and Ultraviolet (UV) degradation during processing and service life (Müller, 2007; Scheirs, 2009).

During production, polymer resin pellets are blended with a masterbatch with carbon black, antioxidants, and stabilizers, then heated and sheared within an extruder. The molten material is directed through extruders and forced through a die. Each manufacturer applies proprietary formulations and processing.

Textured HDPE geomembranes are typically manufactured with three layers (Scheirs, 2009). The primary methods for texturing are flat-die (embossing or structuring), impingement (spray-on texturing), and round-die (coextrusion or blown-film) processes (Hebeler et al., 2005; Müller, 2007; Scheirs, 2009). Figure 1 illustrates these techniques. All can yield single- or double-sided texturing; round-die is the most cost-effective and widely used (Scheirs, 2009).

Most textured HDPE geomembranes used in engineering applications are produced by round-die and flat-die processes (Figure 2). These methods differ in thickness control, especially under aggressive texturing, where round-die products show higher variation (Hsuan et al., 2015). Specifications from the Geosynthetics Research Institute (GRI), such as GRI-GM13 (GRI, 2025a) and GRI-GM42 (GRI, 2025b), do not distinguish between these processes, as both meet requirements with proper quality controls.

The edges of textured geomembrane rolls are usually manufactured with smooth surfaces 10 to 15 cm wide to facilitate seaming and specimen preparation for Stress Cracking Resistance (SCR) testing (Müller, 2007). Recent studies have analyzed performance differences between textured and smooth portions of the same roll (Morsy & Rowe, 2019; Rowe et al., 2020; Zafari, et al., 2023a, b; Aparicio-Ardila, 2025).

Characterizing geomembrane roughness is essential, as asperity spacing, height, and geometry are nonuniformly distributed. Roughness is generally classified into two categories: macroroughness and microroughness (Araújo et al., 2022). Flat-die textured geomembranes may or may not exhibit microroughness. Their macroroughness is often spike-like (Zaharescu, 2018). ASTM D7466 (ASTM, 2015) measures mainly macroroughness and does not explicitly address microroughness.

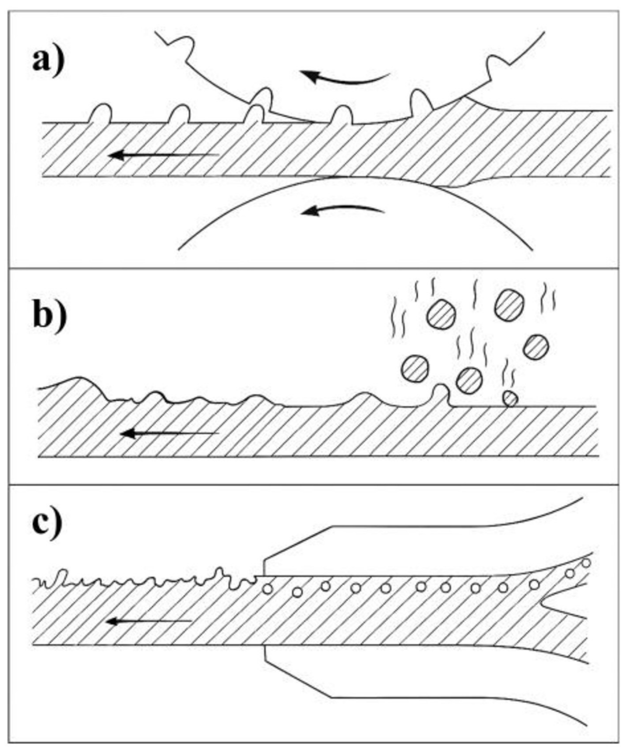

Figure 1. Schematic illustration of the manufacturing processes for textured geomembrane surfaces: (a) flat-die; (b) impingement; (c) round-die. Source: Adapted from Müller (2007).

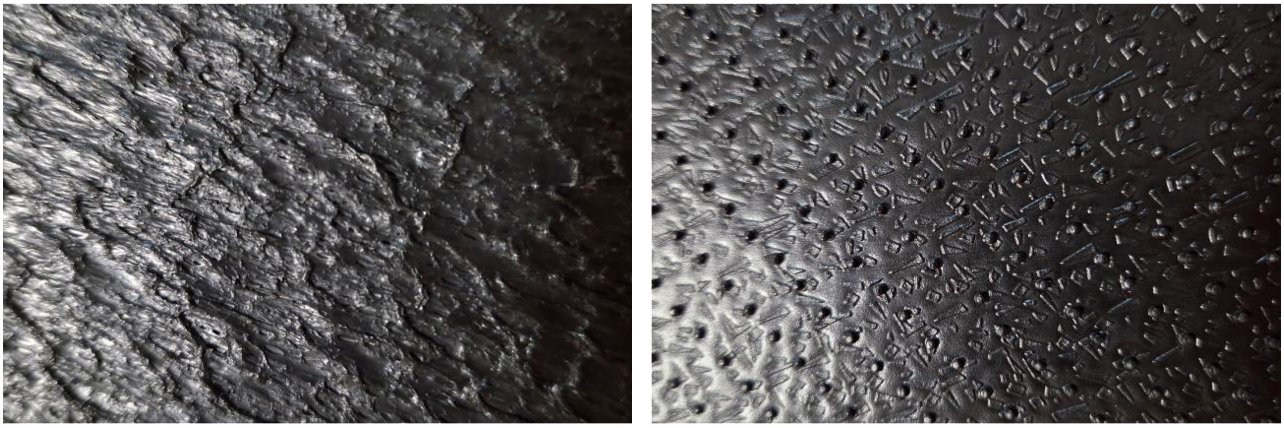

a) b)

Figure 2. Most common textured HDPE geomembranes: (a) round-die; (b) flat-die.

2.2 HDPE geomembranes with advanced technologies

In addition to conventional smooth or textured HDPE geomembranes, several advanced variants are produced. To improve flexibility, some geomembranes are coextruded in a three-layer configuration that combines the chemical resistance of HDPE with the flexibility of LLDPE, typically HDPE/LLDPE/HDPE (Scheirs, 2009).

One well-established technology, recently adopted in Brazil, is the conductive HDPE geomembrane, which features a conductive layer formulated with a different type of carbon black to improve electrical conductivity and facilitate leak detection. According to Scheirs (2009), ensuring continuous conductivity requires a smooth conductive layer, initially limiting texture to the top surface. However, more recent studies report double-sided textured conductive geomembranes, demonstrating technological advancement (Rowe et al., 2020; Zafari et al., 2023b).

Colored HDPE geomembranes, including textured variants, are also available (e.g., Rowe et al., 2020; Aparicio-Ardila et al., 2025a, b). White geomembranes contain titanium dioxide pigments to reduce solar heat gain (Scheirs, 2009).

Another technology is the multilayer HDPE geomembrane with an EVOH core, providing superior gas barrier performance. A typical configuration includes five layers: an outer polyethylene layer (LLDPE or HDPE), a tie layer to bond it to the EVOH, and a central EVOH layer (Di Battista & Rowe, 2020; McWatters et al., 2020). Scheirs (2009) had already described products with similar characteristics, comprising seven to ten layers.

Geomembranes manufactured with PE Raised Temperature resistance (PE-RT) resins show improved tensile property retention, particularly elastic modulus, at temperatures above 60 °C compared to conventional HDPE. Despite the widespread use in piping, few studies address geomembranes (e.g., Clinton & Rowe, 2024).

The GRI-GM42 (GRI, 2025b) specification defines requirements for high-performance HDPE geomembranes, introducing stricter criteria for mechanical, chemical, and UV resistance, as well as a lower thermal expansion coefficient. Applicable to 1.5-3.0 mm geomembranes, it differs from GRI-GM13 (GRI, 2025a) by increasing density from 0.94 to 0.95 g/cm^3, doubling the SCR from 500 to 1000 h, adding the strain-hardening modulus, and making the Standard Oxidative Induction Time (Std-OIT) and High-Pressure Oxidative Induction Time (HP-OIT) mandatory. The break elongation limit for smooth HDPE was reduced; a chlorine-aging test was added; and plaque molding and annealing were standardized.

The GRI continues updating its specifications to incorporate new polyolefin technologies. Addenda under development for GRI-GM13 (GRI, 2025a) and GRI-GM42 (GRI, 2025b) address conductive, colored, and EVOH-layered geomembranes and introduce new tests for colored and graphene-modified HDPE geomembranes.

3. Interface studies

3.1 Interface behavior of textured HDPE geomembranes

Geomembranes are typically in direct contact with other geosynthetics or soil layers. Interface friction is assessed through shear tests to determine the friction angle, a key parameter for slope stability.

Interface shear strength is usually measured using direct shear apparatuses adapted from classical soil mechanics, but with larger shear planes (typically 300 × 300 mm). Smaller devices (e.g., 100 × 100 mm) can be used if validated adequately for the interface (Dixon, 2010).

Several laboratory devices are employed, including direct shear tests (e.g., Costa Junior et al., 2023), inclined plane tests (e.g., Araújo et al., 2022), and ring shear tests (e.g., Xu et al., 2025). Standardized procedures are available, including ASTM D5321 (ASTM, 2012), ISO 12957-1 (ISO, 2018) for direct shear, and ISO 12957-2 (ISO, 2024) for inclined plane tests.

Most published studies focus on the interface between smooth HDPE geomembranes and nonwoven geotextiles, due to their prolonged use in liner systems. For flat-die textured polyethylene geomembranes, studies have analyzed LLDPE interfaces with geotextiles (e.g. Ghazizadeh & Bareither, 2021, 2024) and HDPE with GCLs (e.g. Hanson et al., 2015). Round-die HDPE geomembranes are more frequently investigated due to their wider availability (e.g. Hanson et al., 2015; Lin et al., 2024; Xu & Shi, 2025).

Few studies focus exclusively on flat-die textured geomembranes or compare them with smooth types (e.g. Zaharescu, 2018; Asl Faregh & Hamidi, 2020; Adeleke et al., 2021; Chao et al., 2023; Costa Junior et al., 2023; Lopes & Silva, 2024). These works generally reported that asperity geometry, rather than height alone, governs the interface response, and that flat-die textured surfaces tend to provide lower variability, but similar frictional behavior compared with round-die products.

Overall, these findings underscore the importance of evaluating the interface behavior of textured geomembranes under diverse conditions and with different contact materials. The following section presents studies that compare the interface response of geomembranes produced by different texturing processes.

3.2 Comparative interface studies across different texturing processes

Some studies have examined the interface behavior of textured geomembranes produced using different manufacturing processes (e.g., Hebeler et al., 2005; Costa Junior & Lodi, 2018; Pavanello et al., 2021; Araújo et al., 2022; Xia et al., 2024; Hou et al., 2025).

Hebeler et al. (2005) conducted direct shear tests on geomembrane-geotextile interfaces using 1.5 mm thick flat-die and round-die textured HDPE geomembranes. The tests covered a normal stress between 0.4-312 kPa, showing that round-die geomembranes had stronger peak responses at low stresses but were more prone to wear and strength reduction under shear. In this study no equivalence in asperity height was established.

Costa Junior & Lodi (2018) performed direct shear tests using a small shear box (100 × 100 mm) to investigate soil-geomembrane interfaces involving 2.0 mm thick textured geomembranes manufactured by round-die (asperity height 0.43 mm) and flat-die (asperity height 0.71 mm) processes. Under saturated conditions (water and leachate), the flat-die geomembrane exhibited higher friction angles, which decreased when leachate was present.

Pavanello et al. (2021) carried out inclined plane tests on seven different geosynthetic liner configurations under low normal stress conditions. Tests involving GCLs, geocomposites, and textured geomembranes (flat-die and impingement) identified three sliding mechanisms, sudden, gradual, and uneven, and noted limitations of ISO 12957-2 (ISO, 2024) in representing real kinematic behavior.

Araújo et al. (2022) investigated the influence of micro- and macroroughness parameters on shear resistance through inclined plane tests. Interfaces between soil and geomembranes, as well as geotextile-geomembrane combinations, were analyzed. Using one smooth and three textured (two round-die, one flat-die) geomembranes, the authors observed that higher asperity height in round-die products improved shear resistance.

Xia et al. (2024) conducted interface shear tests between MSW samples of varying ages and textured geomembranes manufactured by flat-die and round-die processes (1.5 mm thick). The internal friction angle increased with MSW age, and the flat-die geomembrane yielded up to 30% higher landfill stability than clay liners.

Hou et al. (2025) examined the interface behavior between different textured HDPE geomembranes and GCL using direct shear tests. The study included one impingement-textured, one round-die, and two flat-die textured geomembranes with varying asperity heights. Flat-die geomembranes exhibited macroroughness only; round-die samples achieved the highest shear strength, while impingement-textured ones showed delamination.

Table 1 summarizes the experimental configurations and resulting interface friction angles reported in the cited studies. No existing study has compared different texturing processes under equivalent asperity heights or standardized roughness metrics, highlighting the need for more controlled investigations.

3.3 Influence of environmental factors on interface performance

The shear behavior at the interface between geosynthetics and soils, or between different geosynthetics, is strongly affected by environmental factors such as temperature, radiation, and exposure to aggressive liquids which are critical for slope stability assessments. Thermal fluctuations, stress redistribution, and post-peak shear mobilization can cause time-dependent deformations even under constant load and temperature (Zamara et al., 2012).

Abdelaal & Solanki (2022) conducted direct shear tests involving HDPE geomembranes, nonwoven geotextiles, and drainage geocomposites. The geomembranes tested included a 1.00 mm thick smooth geomembrane, two flat-die textured geomembranes of 1.5 mm thickness with asperity heights of 0.51 mm and 3.3 mm, and a 2.00 mm thick round-die textured geomembrane with an average asperity height of 0.45 mm. Interface tests were performed using both intact

Table 1. Summary of interface shear strength studies on textured geomembranes.

Reference	Geomembrane Type	Nominal Thickness (mm)	Adjacent Material	Test Type	Normal Stress Range (kPa)	Interface Friction Angle (°)
Hebeler et al. (2005)	Textured HDPE (Round-die)	1.5	Needle-punched nonwoven geotextile (203 g/m²)	Direct Shear Test (102 × 102 mm)	0.4-312	30.4
	Textured HDPE (Flat-die)	1.5				35.1
Costa Junior & Lodi (2018)	Smooth HDPE	2.0	Tropical silty sand-clay soil. Saturated with water and saturated with leachate	Direct Shear Test (100 × 100 mm)	55, 110, 165	8.20 (water saturated) / 7.40 (leachate saturated)
	Textured HDPE (Round-die). Asperity Height 0.43 mm	2.0				21.6 (water saturated) / 15.9 (leachate saturated)
	Textured HDPE (Flat-die). Asperity Height 0.71 mm	2.0				34.5 (water saturated) / 25.7 (leachate saturated)
Pavanello et al. (2021)	HDPE Smooth	2.0	Geocomposite drain with geomat	Inclined Plane Test (1.1 × 0.25 m)	5 (vertical stress)	13.2 (dry) and 10.9 (wet)
	HDPE Textured (Flat-die)	2.0				24.2 (dry)
	HDPE Textured (impingement)	2.0				25 (dry)
Abdelaal & Solanki (2022)	HDPE Smooth	2.0	Nonwoven geotextiles: 200 g/m²(GTX1), 580g/m² (GTX2) and 1500 g/m²(GTX3), and Geocomposite drain with geonet (GCD)	Direct Shear Test (300 × 300 mm)	250, 700, 1000	GTX1: 12.6, GTX2: 12.0, GTX3: 12.0 and GCD:14.0
	Textured HDPE (Round-die). Asperity Height 0.45 mm	2.0	Nonwoven geotextiles: 200 g/m²(GTX1), 580g/m² (GTX2), 1500 g/m²(GTX3) and 2400 g/m²(GTX4), and Geocomposite drain with geonet (GCD)			GTX1: 28.7, GTX2: 21.5, GTX3: 19.8, GTX4: 20.1 and GCD: 24.7
	Textured HDPE (Flat-die). Asperity Height 0.51 mm	1.5	Nonwoven geotextiles: 200 g/m²(GTX1), 580g/m² (GTX2) and 1500 g/m²(GTX3), and Geocomposite drain with geonet (GCD)			GTX1: 32.3, GTX2: 29.5, GTX3: 25.1 and GCD: 29.2
	Textured HDPE (Flat-die). Asperity Height 3.3 mm	1.5	Nonwoven geotextiles: 200 g/m²(GTX1), 580g/m² (GTX2) and 1500 g/m²(GTX3).			GTX1: 34.6, GTX2: 32.5 and GTX3: 30.2.

Table 1. Continued...

Reference	Geomembrane Type	Nominal Thickness (mm)	Adjacent Material	Test Type	Normal Stress Range (kPa)	Interface Friction Angle (°)
Araújo et al. (2022)	HDPE Smooth	2.0	Medium sand; Nonwoven geotextiles: 300 g/m² (GTX1) and 800 g/m² (GTX2)	Inclined Plane Test (1.9 × 0.5 m)	1, 3, 5 (vertical stress)	Sand: ≈ 10 / GTX1: ≈ 12 / GTX2: ≈ 12
	Textured HDPE (Round-die). Asperity Height 0.32 (inner/outer)	2.0				Sand: ≈ 12.5 / GTX1: ≈ 30 / GTX2: ≈ 30
	Textured HDPE (Round-die). Asperity Height 0.67 (inner) / 0.52 (outer)	2.0				Sand: ≈ 12.5 / GTX1: ≈ 64 / GTX2: ≈ 64
	Textured HDPE (Flat-die). Asperity Height 0.78 (inner) / 0.63 (outer)	2.2				Sand: ≈ 12.5 / GTX1: ≈ 42 / GTX2: ≈ 42
Xia et al. (2024)	HDPE Smooth	1.5	MSW of different ages (a): 1.5-2a, 4.5-5a, 8-9a and 10-11a	Direct Shear Test (500 × 500 mm)	50, 100, 200, 400	1.5-2a: ≈ 10 / 4.5-5a: ≈ 14 / 8-9a: ≈ 18 / 10-11a: ≈ 18
	Textured HDPE (Flat-die)	1.5				1.5-2a: ≈ 16 / 4.5-5a: ≈ 22 / 8-9a: ≈ 26 / 10-11a: ≈ 25.5
	Textured HDPE (Round-die)	1.5				1.5-2a: ≈ 14 / 4.5-5a: ≈ 19 / 8-9a: ≈ 25 / 10-11a: ≈ 25
Hou et al. (2025)	HDPE Smooth	2.0	GCL (nonwoven side)	Direct Shear Test (305 × 305 mm)	50, 100, 200, 300, 400	14
	HDPE Textured (impingement). Asperity Height 0.25 mm	2.0				30
	Textured HDPE (Round-die). Asperity Height 0.25 mm	2.0				29
	Textured HDPE (Flat-die). Asperity Height 0.5 mm	1.5				20
	Textured HDPE (Flat-die). Asperity Height 1.5 mm	2.0				38

and aged nonwoven geotextiles that had been immersed for up to two years in either synthetic MSW leachate or chlorinated water at 85 °C. Geomembrane surface hardness was also characterized. The results indicated that increasing the geomembrane asperity height enhanced both peak and large displacement friction angles. However, beyond a certain asperity threshold, further increases produced only marginal improvements. Aged geotextiles (round-die interface) yielded higher shear strengths, indicating that intact-geotextile tests may be conservative.

Material degradation can also influence interface behavior. Xu & Shi (2025) studied the effects of UV radiation on shear behavior and vertical deformation in the interface between a one-sided round-die textured HDPE geomembrane (2.00 mm thick) and a 600 g/m^2 Polyethylene Terephthalate nonwoven geotextile. UV exposure, used to simulate pre-operational conditions, reduced liner compressibility while increasing both peak and large-displacement friction angles, with vertical deformation linked to asperity compression and geotextile deformation.

Temperature also plays a significant role. Chao et al. (2023) investigated interface creep using a large temperature-controlled shear apparatus on silica sand-flat-die geomembrane (2.0 mm) interfaces under varying temperature, normal pressure, and creep loads. The data collected served as input for machine learning models aimed at predicting long-term mechanical behavior. The results indicated that temperature was the most influential factor affecting creep response, followed by loading time.

In a complementary study, Lin et al. (2024) assessed the effect of temperature on shear strength between geotextiles (300 g/m^2) and both round-die smooth and textured HDPE geomembranes through direct shear tests from 10 to 70 °C. Temperature minimally influenced shear curve shape but significantly affected peak and post-peak strength.

Full-scale field tests can offer valuable insights into reinforcement performance that cannot be fully captured by laboratory methods alone. Landfill-scale investigations in the United Kingdom (Zamara et al., 2012) and Italy (Cortellazzo et al., 2022) confirmed the multifaceted environmental effects on geosynthetic interface behavior.

4. Degradation

4.1 Degradation agents

Polymer degradation may compromise the structural integrity and function of geosynthetics, resulting from polymer chain scission induced by environmental agents such as acids, solvents, heat, mechanical stress, UV radiation, water, and oxygen (Palmeira, 2018). Because geosynthetics are often embedded in soil, they experience complex interactions that can accelerate degradation.

Once geosynthetics are installed or put into service, depolymerization processes or significant alterations in mechanical and hydraulic properties may occur when compared to their original characteristics. Correlating individual agents with observed property changes is, however, difficult.

The long-term durability of these materials strongly depends on the composition of the base polymer and the additives included in the formulation. Therefore, polymer degradation analyses must account for both material and environmental parameters. Environmental variables include atmospheric exposure, oxygen availability, fluctuations in relative humidity, chemical composition of the surrounding medium (including pH and metal ions), temperature variation over time, applied mechanical loads, and UV radiation exposure (Lopes & Lopes, 2010).

Temperature (heat) is an agent known to accelerate degradation mechanisms in polymers (Koerner, 2012). It can lead to thermal expansion and, at elevated temperatures, to polymer decomposition. Degradation agents can also interact synergistically, not only among themselves but also with the polymer matrix and its additives. Understanding how multiple degradation agents act concurrently is therefore essential for predicting the service life of HDPE geomembranes and ensuring their long-term performance in geotechnical applications. The following section details the principal degradation mechanisms associated with these agents.

4.2 Degradation mechanisms

4.2.1 Oxidation

Polymer oxidation is a self-catalytic reaction in which oxygen forms free radicals that propagate chain reactions, degrading the polymer structure (Palmeira, 2018).

Oxidative degradation of HDPE geomembranes occurs in three stages. First, antioxidants are depleted through diffusion, extraction, or volatilization. During the induction period, hydroperoxides accumulate until reaching a critical level that accelerates decomposition. In the final stage, molecular and morphological changes cause strength loss and material failure (Rowe & Sangam, 2002; Lopes & Lopes, 2010).

4.2.2 Photodegradation

Photodegradation is mainly caused by solar UV radiation, leading to embrittlement (Brown & Greenwood, 2002). Water interactions, particularly dew, intensify degradation because dissolved oxygen is more reactive than atmospheric oxygen.

Photodegradation is influenced not only by UV intensity but also by temperature, moisture, and atmospheric agents such as ozone, nitrogen oxides, and hydrocarbons. Solar radiation can also raise surface temperatures, further accelerating degradation. Wind or rain abrasion can remove protective layers, exposing fresh surfaces (Elias, 2000).

For polyolefin-based geosynthetics such as PE and PP, stabilizing additives are essential. Antioxidants, HALS, and, primarily, carbon black provide UV protection by absorbing radiation, neutralizing radicals, and improving oxidation resistance, thereby extending durability for decades (Rowe & Sangam, 2002; Lopes & Lopes, 2010).

4.2.3 Chemical degradation

Chemical degradation can occur when geosynthetics are exposed to fluids or waste materials. It is essential to distinguish exposure to acidic or alkaline testing solutions from hydrolysis induced by water (Lopes & Lopes, 2010).

In practice, geomembranes are exposed to various chemicals that may threaten their structural integrity. While single-agent resistance is well documented, performance in complex mixtures remains unpredictable due to synergistic or unknown interactions.

4.2.4 Stress cracking resistance (SCR)

Most organic liquids promote environmental SCR. Brown & Greenwood (2002) identified environmental SCR as a prime example of synergistic polymer failure, requiring both a chemical agent and mechanical stress.

SCR in HDPE geomembranes is critical due to their high crystallinity (40-50%). Although high crystallinity improves stiffness and chemical resistance, it reduces the number of tie molecules, which are essential for ductility and crack resistance (Scheirs, 2009). SCR can occur at stress levels well below the short-term tensile strength. The process has three stages: initial surface cracking, crack growth under sustained stress, and crack propagation leading to multiple fracture paths. Surface scratches, welds, or exposure to detergents and leachates can accelerate it (Rigo & Rollin, 1990; Hsuan, 2000; Rowe & Sangam, 2002).

Field studies show that exposed HDPE geomembranes are particularly vulnerable, with most SCR failures at overlaps or scratches where stresses concentrate. Even minor cracks can compromise liner performance (Rowe, 1998).

4.3 Testing to assess durability

The primary objective of durability assessment in geosynthetics is to define reduction factors that ensure materials achieve the intended design life with the established reliability (ISO 13434, 2020). Durability refers to maintaining functional and mechanical performance under multiple degradation mechanisms (Lopes & Lopes, 2010).

Durability testing methods can be grouped into three categories: accelerated ageing tests conducted in the laboratory, field weathering studies, and service life assessments using exhumed sample analysis (Lopes & Lopes, 2010). Maintaining records of virgin samples installed in the field is essential, as manufacturing processes and formulations evolve, making data obtained for one material difficult to extrapolate to others (ISO, 2020).

To quantify degradation, both polymer microstructural and macrostructural changes in geosynthetic properties must be assessed. Microstructural analysis focuses on molecular-level changes, while macrostructural evaluation considers variations in physical, mechanical, hydraulic, or chemical properties (Lopes & Lopes, 2010). For HDPE geomembranes, common indicators include Oxidation Induction Time (OIT), mechanical strength testing, and SCR.

OIT assesses antioxidant stability; values decrease as antioxidants are consumed. OIT can be measured using Std-OIT (ASTM D3895 or ASTM D8117) (ASTM, 2019, 2021) and HP-OIT (ASTM, 2020a). While Std-OIT is sensitive to phenols and phosphites, HP-OIT detects HALS and thiosynergists. HP-OIT values above 400 minutes typically indicate the presence of HALS (Scheirs, 2009).

ASTM D8117 (ASTM, 2021) revised Std-OIT sample preparation, especially for multilayered geomembranes requiring homogenization, differing from ASTM D3895 (ASTM, 2019). Studies show that antioxidant depletion rates in homogenized samples are comparable to or slower than those in non-homogenized samples (Zafari et al., 2023a, b; Rowe et al., 2025).

Physical and mechanical tests used to evaluate HDPE geomembranes include OIT (Std-OIT and/or HP-OIT), carbon black content (ASTM, 2020b), Melt Flow Index (MFI, ASTM, 2023), and tensile strength and elongation (ASTM, 2020c).

The notched constant tensile load (NCTL) test (ASTM, 2020d) evaluates SCR. Standard practice is to test smooth roll edges or equivalent smooth geomembranes, assuming they represent textured areas. However, recent research shows this may be inaccurate due to differences in properties, degradation rates, manufacturing effects, and other variables (Morsy & Rowe, 2019; Zafari et al., 2023a, b; Abdelaal et al., 2024; Aparicio-Ardila, 2025). New approaches, such as the double-notching method proposed by Abdelaal et al. (2023), along with adjustments to testing parameters, have been developed to provide more accurate assessments of SCR in textured geomembranes. When smooth edges are significantly thinner, testing both regions may offer a more conservative failure estimate (Zafari et al., 2023a).

According to Rigo & Rollin (1990), microstructural analysis provides deeper insights into long-term durability. Palmeira (2018) emphasized thermal properties, including melting temperature, glass transition, and thermal expansion. Chemical characterization methods (Table 2) relate durability to molecular structure and require less material than conventional tests.

TGA and MFI are the most commonly used; additional techniques such as DSC, TMA, and FTIR have also been applied (e.g., Valentin et al., 2018; Lavoie et al., 2021). GC-MS has been used to identify semi-volatile organic compounds in HDPE geomembranes (e.g., Valentin et al., 2022).

Dynamic Mechanical Analysis (DMA) is increasingly used to assess thermal expansion and molecular relaxation in degraded geomembranes, offering insights into structural evolution (e.g., Valentin et al., 2018; Lavoie et al., 2022).

Table 2. Chemical methods to characterize polymeric geomembranes.

Method	Information Obtained	Advantages	Disadvantages
Thermogravimetric Analysis (TGA)	Polymer, additive and ash contents.	Straightforward measurement.	Qualitative results.
	Carbon black amount.	High accuracy.	High cost.
	Decomposition temperatures.	For all polymers.	
Differential Scanning Calorimetry (DSC)	Melting point.	Straightforward measurement.	Qualitative results.
	Crystallinity.	High accuracy.	Limited for chlorinated polymers.
	Oxidation time.	For all polymers.	High cost.
	Glass transition.		
Thermomechanical Analysis (TMA)	Coefficient of linear thermal expansion.	Straightforward measurement.	High cost.
	Softening point.	High accuracy.	
	Glass transition.	For all polymers.	
Infrared spectroscopy (IR), Fourier Transform Infrared Spectroscopy (FTIR) and Attenuated Total Reflectance – Fourier Transform Infrared Spectroscopy (ATR-FTIR)	Identifies additives.	For all polymers.	Specimen preparation. *
	Identify fillers.		No resin information.
	Identify plasticizers.		High cost.
	Rate of oxidation reaction.		
Gas Chromatography-Mass Spectrometry (GC-MS)	Identifies additives.	Straightforward measurement.	Specimen preparation.
	Identify plasticizers.		No resin information.
			High cost.
Density determination	Density.	Straightforward measurement.	Only selected polymers.
	Crystallinity.	Accurate values.	No direct resin information.
		Low cost.	
MFI	Melt index.	Related to molecular weight.	Limited for chlorinated polymers.
	Flow rate ratio.	Straightforward measurement.	Empirical values.
		Low cost.	
Gel Permeation Chromatography (GPC)	Molecular weight distribution.	Accurate values.	Not very common.
		Only valid technique for molecular weight.	Tedious test
		For all polymers.	Specimen preparation.
			Very high cost.

*ATR-FTIR allows measurement to be performed directly on the sample surface without complex preparation. Adapted from Rigo & Rollin (1990).

Some studies have also employed Scanning Electron Microscopy (SEM) to evaluate smooth HDPE geomembranes, enabling detailed surface observation and confirmation of degradation patterns (e.g., Santos, 2014; Noval et al., 2014).

4.4 Service life prediction of textured HDPE geomembranes

Accurately predicting the service life of HDPE geomembranes depends on evaluating exposure conditions and chemical compatibility, as performance varies among environments and formulations. Temperature-dependent degradation testing supports material selection and forecasting (Rowe & Fan, 2024).

Oxidation is widely recognized as the primary degradation mechanism affecting geosynthetics. This process is strongly influenced by UV radiation and occurs in three stages (Section 4.2.1). In Stage I, antioxidant depletion is assessed using OIT tests. Stage II, the induction time, shows measurable reductions in physical or mechanical properties, though still acceptable (typically < 50%). Stage III marks material failure, corresponding to nominal failure or half-life of a key property. (Hsuan & Koerner, 1998; Lopes & Lopes, 2010; Rowe & Sangam, 2002). These three stages are illustrated in Figure 3a.

Stage I is often modelled using an exponential decay function, described by a first-order equation:

$$OIT_t = OIT_0 e^{-st} + y_0 \tag{1}$$

where OIT_t (minutes) represents the oxidation induction time at time t (months), OIT_0 (minutes) is the initial OIT,

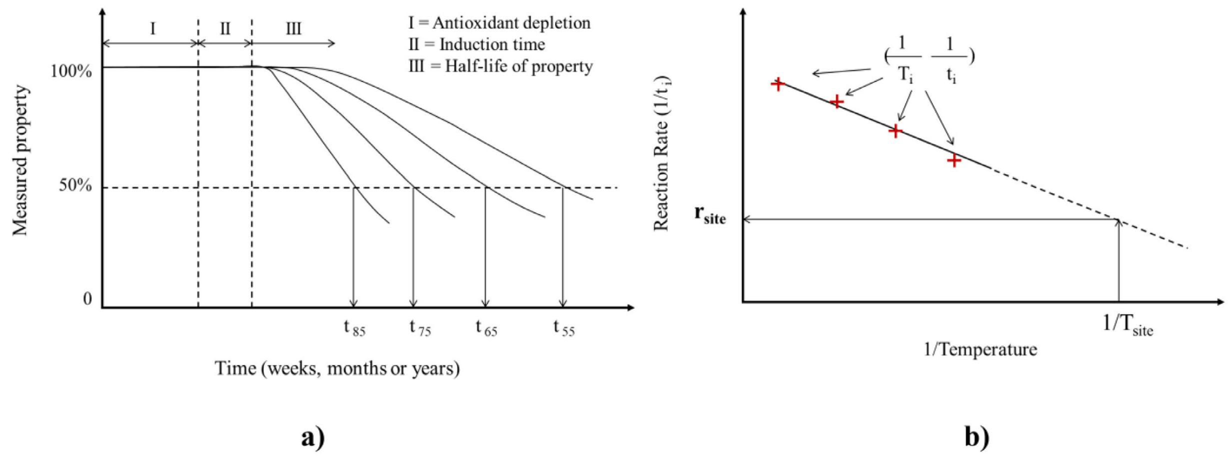

Figure 3. (a) Generalized representation of the three-stage degradation behavior of HDPE geomembranes and the timeline for reaching nominal failure; (b) Procedure for plotting and extrapolating degradation rates using the Arrhenius method to estimate the half-life at a specific field temperature. Source: Adapted from Koerner et al. (2016).

s is the antioxidant depletion rate (month^{-1}), and y_0 is the residual OIT (minutes).

A second-order exponential model may also be applied:

$$OIT_t = A_1 e^{-s_1 t} + A_2 e^{-s_2 t} + y_0 \quad (2)$$

where A_1 and A_2 are fitting constants (minutes), and s_1 and s_2 are the corresponding depletion rates (month^{-1}). The initial OIT value is given by $A_1 + A_2 + y_0$.

Residual Std-OIT thresholds of 3 min or 2-3% of the initial value are typically used to estimate depletion (Abdelaal et al., 2023; Silva et al., 2024).

Service-life models frequently use the Arrhenius equation, which relates the degradation rate to temperature. In Stage I, depletion rates are obtained by fitting OIT data measured at elevated temperatures (e.g., 55, 65, 75, and 95 °C) to exponential models (Equations 1 and 2). These rates are then plotted in an Arrhenius graph, relating the logarithm of the rate to inverse temperature, enabling extrapolation to field conditions (Figure 3b). Stage III follows a similar procedure using mechanical degradation data (e.g., tensile strength, elongation at break, or SCR). Stage II corresponds to the time between antioxidant depletion and the onset of measurable property loss (Silva et al., 2024; Koerner et al., 1992, 2016).

The Arrhenius approach enables time-temperature extrapolation, with predicted service lives ranging from a few years to millennia, depending on material properties and exposure (Koerner et al., 2016; Rowe & Sangam, 2002).

Service life is also affected by tensile stress and weld quality. To minimize stress, strain should stay below 3% (Rowe & Yu, 2019), and installation and welding must follow proper procedures.

There is a clear distinction between the lifespan of exposed versus buried HDPE geomembranes. Exposed HDPE geomembranes typically last 50 to 70 years, whereas buried ones, protected from environmental agents, may remain functional for centuries or millennia (Rowe & Fan, 2024). According to Koerner et al. (2016), buried geomembranes last about 7 times as long.

Textured HDPE geomembranes differ from smooth ones due to lower tensile strength and elongation for the same thickness, yet their stress-strain curves remain comparable up to yield. Despite reduced tensile strength and elongation, their initial stress–strain response is similar, allowing equivalent performance when yield governs (Scheirs, 2009). However, recent research indicates that texturing may accelerate or delay antioxidant depletion (e.g., Morsy, 2019; Morsy & Rowe, 2019; Rowe et al., 2025).

Although predictive models support long-term assessment, the unique features of textured geomembranes, manufacturing, morphology, and mechanics demand specific durability evaluations, as discussed in the next section.

5. Durability studies of textured HDPE geomembranes

5.1 Laboratory and field investigations

Although limited, laboratory studies evaluating the durability of textured HDPE geomembranes have focused on degradation mechanisms, such as UV ageing in a chamber and immersion in synthetic MSW leachate or synthetic Low-Level Waste (LLW) leachate.

Regarding UV chamber ageing using 20 h UV + 4 h condensation cycles, Lodi (2003) tested a double-sided white/black textured HDPE geomembrane for six months, observing 34% Std-OIT and 57% strain-at-break reduction. More recently, Aparicio-Ardila et al. (2025a) and Aparicio-Ardila (2025) used the same UV chamber, applying shorter exposure times and higher temperatures as per GRI-GM13 (GRI, 2025a). Aparicio-Ardila et al. (2025a) tested three double-sided textured HDPE geomembranes (white/black, green/green, black/black) with a thickness of 1.00 mm. Results showed that colored surfaces depleted antioxidants faster than conventional black textured HDPE. Strain at break remained the most affected property, with high variability, typical of textured geomembranes (Zafari et al., 2023a).

Both Lodi (2003) and Aparicio-Ardila et al. (2025a) used flat-die products. Aparicio-Ardila (2025) compared 2 mm double-sided black textured geomembranes manufactured by flat-die and round-die processes, including smooth edges. Smooth edges showed higher antioxidant depletion due to reduced thickness, and variability was greater in round-die samples.

Morsy (2019) and related studies (Morsy & Rowe, 2017, 2019, 2020; Rowe et al., 2025) examined 1.5 mm round-die double-sided textured HDPE immersed in synthetic MSW leachate (40-85 °C). The textured surface showed ≈ 15% faster depletion (3-8 months) and up to 40% Std-OIT loss (34 months), but SCR was unaffected. Rowe et al. (2025) confirmed faster degradation in textured regions after 62 months.

Morsy & Rowe (2020) evaluated SCR for samples exposed for 8 and 16 months at 85 °C, concluding that surface discontinuities and thickness variation drove SCR variability, making textured geomembranes more susceptible to SCR.

Abdelaal et al. (2024), Rowe et al. (2020), and Zafari et al. (2023a, b) evaluated double-sided and one-sided white/black textured HDPE geomembranes with their smooth edges or smooth equivalents. Zafari et al. (2023a, b) and Abdelaal et al. (2024) immersed these geomembranes in synthetic MSW leachate for up to 50 months at varied temperatures.

Zafari et al. (2023a) reported color and thickness differences between smooth edges and textured zones. They found that texturing may accelerate or delay antioxidant depletion depending on the material. Smooth edges degraded tensile break properties faster due to a thinner core, despite faster antioxidant depletion in textured areas. SCR showed the earliest nominal failure. Abdelaal et al. (2024) proposed a double-notch SCR method for textured multilayer geomembranes, noting that smooth edges may under- or overestimate degradation.

Rowe et al. (2020) and Zafari et al. (2023b, 2024) also studied geomembranes with conductive layers. Zafari et al. (2023b) observed that the conductive layer could either accelerate or inhibit depletion; delamination occurred under aggressive ageing, but should not be generalized. Rowe et al. (2020) and Zafari et al. (2024) compared exposure to LLW (pH 7-9) and synthetic MSW, finding slightly faster depletion at pH 9 and ~ 20% longer time-to-failure in LLW leachate due to fewer surfactants. A synthesis of these findings is shown in Table 3.

A field durability study involving the deliberate exposure of textured HDPE geomembranes was reported by Aparicio-Ardila et al. (2025b). The study evaluated 1.00 mm double-sided colored textured HDPE geomembranes (white/black, green/green, black/black), manufactured by flat-die and exposed to natural weathering in southern Brazil for 8.5 to 10.5 years, using original unexposed samples as references. The white/black geomembrane with the white side exposed for 9 years showed the most severe degradation despite a shorter exposure than the green/green sample.

5.2 Performance of exhumed textured HDPE geomembranes

Exhumation usually occurs during repairs or expansions, verifying if exposed or buried geomembranes retain adequate properties for reuse and weldability (Aparicio-Ardila, 2025; Rafter et al., 2018).

Accurate assessment requires Manufacturing Quality Control (MQC) data to establish baseline properties. These values should be recorded during Construction Quality Control (CQC) by the installers, but they are not always available. As a result, many exhumation studies compare exposed samples to ‘typical’ values or GRI-GM13 (GRI, 2025a) specification (e.g., Lavoie et al., 2022; Rowe & Ewais, 2015; Rowe et al., 2003; Urashima et al., 2024). Even more reliable comparisons can be made when it is possible to obtain an original, properly stored sample, either from the manufacturer’s archive or the project owner, for direct benchmarking against exhumed material.

Exhumation data for textured geomembranes remain scarce (e.g. Aparicio-Ardila, 2025; Benson, et al., 2010; Koerner & Koerner, 2019; Rafter et al., 2018). Benson et al. (2010) studied textured LLDPE geomembranes exhumed after 4.7-5.8 years in a U.S. landfill. The 1 mm round-die product showed stable MFI and OIT values but ~20% lower tensile yield strength.

Rafter et al. (2018) and Koerner & Koerner (2019) conducted exhumations of landfill base liner systems that had been in operation for 22 and 23 years, respectively. Both studies included 1.5 mm round-die double-sided textured HDPE geomembranes and extrusion weld samples (Figure 4). The authors found that weld strength and the geomembrane’s physical and mechanical properties remained above specification references.

Aparicio-Ardila (2025) exhumed flat-die double-sided textured HDPE geomembranes (2.00 mm) from landfill covers and a zinc mining dam in Brazil. Landfill cover samples were in service for 3.2 and 4.5 years in São Paulo and Rio de Janeiro states. A notable aspect of this study is that original reference samples were traced using installation as-built records. Depletion of antioxidants was higher in the São Paulo sample, despite shorter exposure. Differences in property reduction were also found between the textured and smooth portions. In the mining dam samples (bottom and slope), exposed for approximately 20 years, reference samples were unavailable, so properties were compared to GRI-GM13 (GRI, 2025a). Bottom samples (covered by tailings) retained higher Std-OIT than slope samples (UV-exposed). The slope textured area showed Std-OIT six times lower than its smooth edge. The smooth edge failed the strain-at-break reference (GRI-GM13,GRI, 2025a) for smooth geomembranes, but exceeded the textured

Table 3. Summary of textured HDPE geomembrane durability research (Laboratory).

Reference	Material Used	Core thickness	Fabrication	Exposure Type	Exposure Time and Temperature	Tests Performed
Lodi (2003)	Double-sided white/black textured HDPE GMB.	1.0 mm	flat-die	Exposure in fluorescent UV chamber (controlled cycles of radiation and condensation).	6 months (75 °C UV, 60 °C condensation).	Antioxidant Depletion (Std-OIT). Tensile Properties. TMA. Tear Resistance.
Morsy & Rowe (2017)	Double-sided black textured HDPE. Included smooth edges.	1.5 mm	round-die	Immersion in synthetic MSW leachate, in forced air ovens.	Preliminary results, 3 to 8 months. (75 and 85 °C).	Antioxidant Depletion (Std-OIT and HP-OIT). MFI. Tensile Properties.
Morsy & Rowe (2019)	Double-sided black textured HDPE. Included smooth edges or smooth equivalents.	1.5 mm	round-die	Immersion in simulated MSW leachate.	34 months. (40, 55, 75, and 85 °C).	Antioxidant Depletion (Std-OIT and HP-OIT). HLMI. Tensile Properties. SCR.
Morsy & Rowe (2020)	Double-sided black textured HDPE. Included smooth edges.	1.5 mm	round-die	Accelerated aging by immersion in synthetic MSW leachate.	8 and 16 months. 85 °C.	SCR. Stress Intensity Factor (KI) and Crack Propagation Rate (da/dt). Scanning Electron Microscopy (SEM).
Rowe et al. (2020)	Double-sided white/black textured HDPE. Included smooth edges or smooth equivalents. Some were conductive.	2.07 to 2.66 mm	round-die	Immersion in simulated MSW leachate and two LLW leachates with pH 7 and pH 9.	34 months (40-85 °C).	Antioxidant Depletion (Std-OIT and HP-OIT). Tensile Properties. SCR on smooth edges/equivalent smooth.
Zafari et al. (2023a)	Double-sided and one -side white/ black textured HDPE. Included smooth edges.	2.0 mm	round-die	Immersion in synthetic MSW leachate.	50 months (40, 55, 65, 75, 85 °C).	Antioxidant Depletion (Std-OIT and HP-OIT). Tensile Properties. SCR on smooth edges.
Zafari et al. (2023b)	Double-sided and one -side white/ black textured HDPE. Included smooth edges. Some were conductive.	2.0 mm	round-die	Oven immersion in synthetic MSW leachate.	50 months (40, 55, 65, 75, 85 °C).	Antioxidant Depletion (Std-OIT and HP-OIT). Tensile Properties. SCR on smooth edges/equivalent smooth.
Abdelaal et al. (2024)	Double-sided textured HDPE geomembranes. Included smooth edges or smooth equivalents. Some were conductive.	2.07 to 2.66 mm	round-die	Immersion in synthetic MSW leachate.	50 months. (55°C and 85 °C)	SCR. MFI. Tensile break properties (strength and elongation). For SCR, the effect of notch direction, notch depth, and applied nominal stresses were analyzed.
Rowe et al. (2025)	Double-sided black textured HDPE. Included smooth edges or smooth equivalents.	1.5 mm	round-die	Immersion in synthetic MSW leachate.	96 months (40, 55, 65, 75, 85 °C).	Antioxidant Depletion (Std-OIT, HP-OIT). MFI. Tensile Properties (break strength and strain). SCR.
Zafari et al. (2024)	Double-sided textured HDPE geomembranes. Included smooth edges or smooth equivalents. Some conductive.	2.07 to 2.66 mm	round-die	Immersion in two LLW leachates with pH 7 and pH 9.	48-55 months (40-85 °C).	Antioxidant Depletion (Std-OIT and HP-OIT). Tensile Properties. SCR on smooth edges/equivalent smooth.
Aparicio-Ardila et al. (2025a)	Double-sided colored textured HDPE (white/black, green/green, black/black).	1.0 mm	flat-die	Exposure in fluorescent UV chamber (controlled cycles of radiation and condensation).	500, 1000, and 2000 hours (75 °C UV, 60 °C condensation).	Antioxidant Depletion (Std-OIT). MFI. Tensile Properties. Secant Rigidity Modulus.
Aparicio-Ardila (2025)	Double-sided black textured HDPE. Included smooth edges.	2.0 mm	flat-die and round-die	Exposure in fluorescent UV chamber (controlled cycles of radiation and condensation).	500, 1000, and 2000 hours (75 °C UV, 60 °C condensation).	Antioxidant Depletion (Std-OIT). MFI. Tensile Properties.

geomembranes reference by 213%. This highlights uncertainty about which specification reference should apply to smooth edges of textured geomembranes.

Overall, exhumation studies, though few, provide valuable long-term field evidence. They emphasize the need to consider surface morphology, exposure, and installation context when assessing degradation, and the importance of original reference samples for reliable evaluation.

6. Installation

As previously discussed, installation practices are crucial to the long-term durability of geomembrane systems; poor welding can create stress, weaknesses, or defects.

For HDPE geomembranes, two primary welding methods are used: extrusion welding (Figure 4b), which uses a filler rod, and hot wedge welding (Figures 5a and 5b) the

a) b)

Figure 4. Field exhumation procedures conducted by Rafter et al. (2018): (a) extraction of HDPE geomembrane sheet samples; (b) sampling of extrusion welds.

a) b) c)

Figure 5. CQC testing on flat-die textured HDPE geomembrane: (a) air pressure testing on hot wedge weld with textured-to-textured overlap; (b) air pressure testing on hot wedge weld with smooth-to-smooth edge overlap; (c) vacuum box testing on extrusion weld.

predominant field welding. Extrusion welding is typically reserved for detailed work, such as repairs or extrusion patches, and connections to structures like pipes.

Quality control of welded seams must be ensured through Construction Quality Control (CQC). Non-destructive testing methods for CQC include air channel pressure testing (ASTM, 2018a) for hot wedge welding (Figures 5a and 5b) and vacuum box testing (ASTM, 2016) for extrusion welding (Figure 5c). Spark testing (ASTM, 2018b), using a conductive copper wire, can also be applied to verify the integrity of extrusion welding.

Destructive testing (ASTM, 2018c) is required for both welding types and must meet minimum shear and peel strength values defined in GRI-GM19a (GRI, 2021) specification. Reference seam strength values are now appended to GRI-GM13 (GRI, 2025a) and GRI-GM42 (GRI, 2025b) specifications, as GRI-GM19a (GRI, 2021) will be deprecated in 2026.

Several guidelines outline best practices for HDPE geomembrane installation (e.g. DVS, 2019; IAGI, 2015; Toepfer, 2015). In Brazil, installation follows ABNT NBR 16199 (ABNT, 2020), currently under its second revision.

The skill and qualification of welders are essential for achieving high-quality seams. Currently, the Certified Welding Technician (CWT) program, developed by the International Association of Geosynthetic Installers (IAGI), is the only internationally recognized certification for geomembrane installers. This program ensures that welders possess the necessary experience, technical competence, and understanding of industry standards required to perform reliable and durable welds.

Effective CQC relies on the use of high-quality geomembranes. To ensure this, both CQC and MQC are subject to independent oversight through Construction Quality Assurance (CQA) and Manufacturing Quality Assurance (MQA), respectively. MQA verifies that the geomembranes delivered to the construction site conform to the specified requirements, typically through testing conducted by accredited third-party laboratories (Scheirs, 2009).

An independent consultant or team must perform CQA and MQA. CQA may also involve geoelectrical leak-detection methods during construction and maintenance to reduce undetected leaks and improve system integrity (Müller, 2007; Giroud, 2016; Zidan et al., 2024).

7. Conclusion

Based on the comprehensive literature review conducted on textured HDPE geomembranes, the following conclusions can be drawn:

- There is no definitive evidence that flat-die or round-die textured HDPE geomembranes perform better in geotechnical and environmental engineering applications. Each process yields materials with distinct surface profiles, and performance varies with site and design conditions. Batch-to-batch variability is also significant;
- Regarding interface behavior, no published study has systematically compared textured HDPE geomembranes from different manufacturing methods while controlling asperity height or roughness parameters. Future work should isolate these factors to quantify better how manufacturing affects interface performance;
- Interface shear strength and deformation behavior are strongly influenced by temperature, chemical exposure, UV radiation, and ageing. These interdependent environmental factors must be incorporated into design and material selection;
- An integrated approach combining laboratory, numerical, and field data is essential for realistic interface performance predictions and improved long-term reliability of barrier systems;
- The service life of HDPE geomembranes depends on environmental and mechanical interactions, including tensile stress and weld quality. Textured geomembranes offer frictional gains but may reduce mechanical strength, requiring specific testing and design attention;
- Laboratory, field, and exhumation studies on textured geomembranes remain limited; expanding them is vital to advance understanding of degradation mechanisms and durability;
- Field data complement laboratory findings. More standardized exhumation studies are needed to refine durability predictions and support practice;
- Standardized accelerated durability tests remain essential for assessing long-term HDPE behavior. As manufacturing evolves, material specifications must be updated with compatible welding protocols and validated through long-term field performance studies.

Acknowledgements

The authors express their gratitude to the Geosynthetics Laboratory of the Geotechnical Department at the School of Engineering of São Carlos, University of São Paulo. To MSc. Clever A. Valentin and PhD. Marcelo Kobelnik. The authors also thank Tecnoplas Engenharia for providing the CQC testing photographs.

Declaration of interest

The authors have no conflicts of interest to declare. All co-authors have observed and affirmed the contents of the paper and there is no financial interest to report.

Authors' contributions

Maria Alejandra Aparicio-Ardila: formal analysis, conceptualization, methodology, data, validation, formal analysis, visualization, writing – original draft and review. Jefferson Lins

da Silva: supervision, conceptualization, data curation, formal analysis, validation, writing – original draft and review.

Data availability

The datasets generated analyzed in the course of the current study are available from the corresponding author upon request.

Declaration of use of generative artificial intelligence

This work was prepared without the assistance of generative artificial intelligence (GenAI).

List of symbols and abbreviations

s	antioxidant depletion rate (month^{-1})
s_1	antioxidant depletion rate (month^{-1})
s_2	antioxidant depletion rate (month^{-1})
t	Time (months)
y_0	residual Oxidative Induction Time (minutes)
A_1	fitting constant (minutes)
A_2	fitting constant (minutes)
ABNT NBR:	Brazilian Technical Standard
ASTM	American Society for Testing and Materials
ATR-FTIR:	Attenuated Total Reflectance Fourier Transform Infrared Spectroscopy
CQA	Construction Quality Assurance
CQC	Construction Quality Control
CWT	Certified Welding Technician
DMA	Dynamic Mechanical Analysis
DSC	Differential Scanning Calorimetry
DVS	Deutscher Verband für Schweissen und Verwandte Verfahren E.V.
EVOH	Ethylene Vinyl Alcohol
FTIR	Fourier Transform Infrared Spectroscopy
GCL	Geosynthetic Clay Liner
GC-MS	Gas Chromatography–Mass Spectrometry
GPC	Gel Permeation Chromatography
GRI	Geosynthetic Research Institute
HALS	Hindered Amine Light Stabilizers
HDPE	High-Density Polyethylene
HP-OIT	High-Pressure Oxidative Induction Time
IAGI	International Association of Geosynthetic Installers
IR	Infrared Spectroscopy
ISO	International Organization for Standardization
LLDPE	Linear Low-Density Polyethylene
LLW	Low-Level Waste
MFI	Melt Flow Index
MQA	Manufacturing Quality Assurance
MQC	Manufacturing Quality Control
MSW	Municipal Solid Waste
NCTL	Notched Constant Tensile Load
OIT	Oxidative Induction Time
OIT_t	oxidative induction time at time t (minutes)
OIT_0	initial Oxidative Induction Time (minutes)
PE	Polyethylene
PE-RT	Polyethylene raised temperature resistance
PP	Polypropylene
SCR	Stress Cracking Resistance
SEM	Scanning Electron Microscopy
Std-OIT	Standard Oxidative Induction Time
TGA	Thermogravimetric Analysis
TMA	Thermomechanical Analysis
UV	Ultraviolet

References

Abdelaal, F.B., & Solanki, R. (2022). Effect of geotextile ageing and geomembrane surface roughness on the geomembrane-geotextile interfaces for heap leaching applications. *Geotextiles and Geomembranes*, 50(1), 55-68. https://doi.org/10.1016/j.geotexmem.2021.09.001.

Abdelaal, F.B., Rowe, R.K., Morsy, M.S., & Silva, R.A. (2023). Degradation of HDPE, LLDPE, and blended polyethylene geomembranes in extremely low and high pH mining solutions at 85° C. *Geotextiles and Geomembranes*, 51(5), 27-38. https://doi.org/10.1016/j.geotexmem.2023.04.011.

Abdelaal, F.B., Zafari, M., & Rowe, R.K. (2024). Assessment of the stress crack resistance of multilayered textured HDPE geomembranes. *Geosynthetics International*, 31(6), 1-15. https://doi.org/10.1680/jgein.23.00096.

ABNT NBR 16199. (2020). *Barreiras geossintéticas: instalação de geomembranas poliméricas*. ABNT - Associação Brasileira de Normas Técnicas, Rio de Janeiro, RJ (in Portuguese).

Adeleke, D., Kalumba, D., Nolutshungu, L., Oriokot, J., & Martinez, A. (2021). The influence of asperities and surface roughness on geomembrane/geotextile interface friction angle. *International Journal of Geosynthetics and Ground Engineering*, 7(2), 20. https://doi.org/10.1007/s40891-021-00265-y.

Aparicio-Ardila, M.A. (2025). *Durability of textured HDPE geomembranes in environmental protection applications* [Doctoral thesis]. Escola de Engenharia de São Carlos, Universidade de São Paulo.

Aparicio-Ardila, M.A., Valentin, C.A., & Silva, J.L. (2025a). Colored HDPE textured geomembranes exposed to UV: laboratory insights into material degradation. *International Journal of Geosynthetics and Ground Engineering*, 11(3), 23. https://doi.org/10.1007/s40891-025-00632-z.

Aparicio-Ardila, M.A., Kobelnik, M., Valentin, C.A., Palomino, C.F., Sabogal-Paz, L.P., & Silva, J.L. (2025b). Natural weathering effects on white, green, and black HDPE textured GMs. *Geosynthetics International*, 32(6), 1-40. https://doi.org/10.1680/jgein.24.00150.

Araújo, G.L.S., Sánchez, N.P., Palmeira, E.M., & Almeida, M.G.G. (2022). Influence of micro and macroroughness of geomembrane surfaces on soil-geomembrane and geotextile-geomembrane interface strength. *Geotextiles and Geomembranes*, 50(4), 751-763. https://doi.org/10.1016/j.geotexmem.2022.03.015.

Asl Faregh, A.H., & Hamidi, A. (2020). Impact of inherent anisotropy on the shear behavior of sand-textured geomembrane interface. *International Journal of Civil Engineering*, 18(10), 1113-1123. https://doi.org/10.1007/s40999-020-00519-2.

ASTM D5321. (2012). *Standard test method for determining the shear strength of soil-geosynthetic and geosynthetic-geosynthetic interfaces by direct shear.* ASTM International, West Conshohocken, PA.

ASTM D7466. (2015). *Standard test method for measuring the asperity height of textured geomembrane.* ASTM International, West Conshohocken, PA.

ASTM D5641. (2016). *Standard practice for geomembrane seam evaluation by vacuum chamber.* ASTM International, West Conshohocken, PA.

ASTM D5820. (2018a). *Standard practice for pressurized air channel evaluation of dual-seamed geomembranes.* ASTM International, West Conshohocken, PA.

ASTM D6365. (2018b). *Standard practice for nondestructive testing of geomembrane seams using the spark test.* ASTM International, West Conshohocken, PA.

ASTM D6392. (2018c). *Standard test method for determining the integrity of nonreinforced geomembrane seams produced using thermo-fusion methods.* ASTM International, West Conshohocken, PA.

ASTM D3895. (2019). *Standard test method for oxidative-induction time of polyolefins by differential scanning calorimetry.* ASTM International, West Conshohocken, PA.

ASTM D5885. (2020a). *Standard test method for oxidative induction time of polyolefin geosynthetics by high-pressure differential scanning calorimetry.* ASTM International, West Conshohocken, PA.

ASTM D4218. (2020b). *Standard test method for determination of carbon black content in polyethylene compounds by the muffle-furnace technique.* ASTM International, West Conshohocken, PA.

ASTM D6693. (2020c). *Standard test method for determining tensile properties of nonreinforced polyethylene and nonreinforced flexible polypropylene geomembranes.* ASTM International, West Conshohocken, PA.

ASTM D5397. (2020d). *Standard test method for evaluation of stress crack resistance of polyolefin geomembranes using notched constant tensile load test.* ASTM International, West Conshohocken, PA.

ASTM D8117. (2021). *Standard test method for oxidative induction time of polyolefin geosynthetics by differential scanning calorimetry.* ASTM International, West Conshohocken, PA.

ASTM D1238. (2023). *Standard test method for melt flow rates of thermoplastics by extrusion plastometer.* ASTM International, West Conshohocken, PA.

Benson, C.H., Kucukkirca, I.E., & Scalia, J. (2010). Properties of geosynthetics exhumed from a final cover at a solid waste landfill. *Geotextiles and Geomembranes*, 28(6), 536-546. https://doi.org/10.1016/j.geotexmem.2010.03.001.

Brown, R., & Greenwood, J.H. (2002). *Practical guide to the assessment of the useful life of plastics*. Shropshire: Smithers Rapra Publishing.

Cardoso, R., Calcina, A., Oliveira, C., Carvalho, A.H., & Sarlo, R.J. (2010). Utilização de geomembrana de PEAD em tratamento de fundação na barragem de São Salvador. In *Anais do Congresso Brasileiro de Mecânica dos Solos e Engenharia Geotécnica (COBRAMSEG)*, Gramado, RS (in Portuguese).

Chao, Z., Wang, H., Hu, H., Ding, T., & Zhang, Y. (2023). Predicting the temperature-dependent long-term creep mechanical response of silica sand-textured geomembrane interfaces based on physical tests and machine learning techniques. *Materials*, 16(18), 6144. https://doi.org/10.3390/ma16186144.

Clinton, M., & Rowe, R.K. (2024). Long-term durability of two HDPE geomembranes formulated with polyethylene of raised temperature resistance (PE-RT). *Geotextiles and Geomembranes*, 52(3), 304-318. https://doi.org/10.1016/j.geotexmem.2023.11.003.

Cortellazzo, G., Russo, L.E., Busana, S., Carbone, L., Favaretti, M., & Hangen, H. (2022). Field trial of a reinforced landfill cover system: performance and failure. *Geotextiles and Geomembranes*, 50(4), 655-667. https://doi.org/10.1016/j.geotexmem.2022.03.007.

Costa Junior, S.L., & Lodi, P.C. (2018). Assessment of the interface shear strength between HDPE geomembrane and tropical soil by the direct shear test. Proc. 11th International Conference on Geosynthetics 2018, ICG 2018.

Costa Junior, S.L., Aparicio-Ardila, M.A., Palomino, C.F., & Lins da Silva, J. (2023). Analysis of textured geomembrane-soil interface strength to mining applications. *International Journal of Geosynthetics and Ground Engineering*, 9(1), 3. https://doi.org/10.1007/s40891-022-00423-w.

Di Battista, V., & Rowe, R.K. (2020). TCE and PCE diffusion through five geomembranes including two coextruded with an EVOH layer. *Geotextiles and Geomembranes*, 48(5), 655-666. https://doi.org/10.1016/j.geotexmem.2020.03.010.

Dixon, N. (2010). Soil-geosynthetic interaction: interface behaviour. In *Proceedings of the 9th International Conference on Geosynthetics (ICG 2010).* Universidade do Porto.

DVS. (2019). *DVS 2225-4: Welding of lining membranes made of polyethylene (PE) for the sealing of landfill and contaminated sites.* DVS Media GmbH, Düsseldorf.

Elias, V. (2000). *Mechanically stabilized earth walls and reinforced soil slopes design & construction guidelines.* Washington, D.C.: U.S. Department of Transportation.

Gardoni, M.G., Palmeira, E.M., Almeida, M., Araújo, G.L.S., Ehrlich, M., Riccio, M., Santos, E.C.G., & Vilar, O.M. (2025). Geosynthetics in Brazil: historical overview and future developments. *Soils and Rocks*, 48(3), e2025011224. https://doi.org/10.28927/SR.2025.011224.

Ghazizadeh, S., & Bareither, C.A. (2021). Failure mechanisms of geosynthetic clay liner and textured geomembrane composite systems. *Geotextiles and Geomembranes*, 49(3), 789-803. https://doi.org/10.1016/j.geotexmem.2020.12.009.

Ghazizadeh, S., & Bareither, C.A. (2024). Effect of temperature on critical strength of geosynthetic clay liner/textured geomembrane composite systems. *Geotextiles and Geomembranes*, 52(1), 12-26. https://doi.org/10.1016/j.geotexmem.2023.08.005.

Giroud, J.P. (2016). Leakage control using geomembrane liners. *Soils and Rocks*, 39(3), 213-235. https://doi.org/10.28927/SR.393213.

GRI GM19a. (2021). *Standard specification for seam strength and related properties of thermally bonded homogeneous polyolefin geomembranes/barriers.* Geosynthetic Research Institute, Folsom, PA.

GRI GM13. (2025a). *Standard specification for test methods, test properties and testing frequency for high density polyethylene (HDPE) smooth and textured GMs.* Geosynthetic Research Institute, Folsom, PA.

GRI GM42. (2025b). *Standard specification for test methods, test properties and testing frequency for high density polyethylene (HDPE) geomembrane used in extreme conditions.* Geosynthetic Research Institute, Folsom, PA.

Hanson, J.L., Chrysovergis, T.S., Yesiller, N., & Manheim, D.C. (2015). Temperature and moisture effects on GCL and textured geomembrane interface shear strength. *Geosynthetics International*, 22(1), 110-124. https://doi.org/10.1680/gein.14.00035.

Hebeler, G., Frost, J.D., & Myers, A. (2005). Quantifying hook and loop interaction in textured geomembrane geotextile systems. *Geotextiles and Geomembranes*, 23(1), 77-105. https://doi.org/10.1016/j.geotexmem.2004.06.002.

Hou, J., Xie, X., & Benson, C.H. (2025). Effect of geomembrane texturing method on geomembrane-dry GCL interface shear behavior. *Geotextiles and Geomembranes*, 53(6), 1185-1199. https://doi.org/10.1016/j.geotexmem.2025.05.008.

Hsuan, Y.G. (2000). Data base of field incidents used to establish HDPE geomembrane stress crack resistance specifications. *Geotextiles and Geomembranes*, 18(1), 1-22. https://doi.org/10.1016/S0266-1144(99)00018-7.

Hsuan, Y.G., & Koerner, R.M. (1998). Antioxidant depletion lifetime in high density polyethylene geomembranes. *Journal of Geotechnical and Geoenvironmental Engineering*, 124(6), 532-541. https://doi.org/10.1061/(ASCE)1090-0241(1998)124:6(532).

Hsuan, Y.G., Koerner, R.M., & Koerner, G.R. (2015). *Rationale and background for the GRI-GM13 specification for HDPE geomembranes* (GSI White Paper, No. 32). Folsom: Geosynthetic Research Institute.

International Association of Geosynthetic Installers – IAGI. (2015). *HDPE and LLDPE geomembrane installation specification*. Littleton: IAGI.

ISO 12957-1. (2018). *Geosynthetics. Determination of friction characteristics. Part 1: direct shear test.* International Organization for Standardization, Geneva.

ISO TS 13434. (2020). *Geosynthetics: guidelines for the assessment of durability.* International Organization for Standardization, Geneva.

ISO 12957-2. (2024). *Geosynthetics: determination of friction characteristics. Part 2: inclined plane test.* International Organization for Standardization, Geneva.

Jucá, J.F., Norberto, A., Santos Júnior, J.I., & Marinho, F. (2021). Brasília municipal solid waste landfill: a case study on flow and slope stability. *Soils and Rocks*, 44(3), 1-13. https://doi.org/10.28927/SR.2021.067321.

Koerner, G.R., & Koerner, R.M. (2019). Case history of an exhumed landfill double liner system. In *Proceedings of the Eighth International Conference on Case Histories in Geotechnical Engineering* (pp. 22-32). ASCE. https://doi.org/10.1061/9780784482148.003.

Koerner, R.M., Hsuan, Y.G., & Koerner, G.R. (2016). Lifetime predictions of exposed geotextiles and geomembranes. *Geosynthetics International*, 24(2), 198-212. https://doi.org/10.1680/jgein.16.00026.

Koerner, R.M. (2012). *Designing with geosynthetics* (Vol. 1). Bloomington: Xlibris Corporation.

Koerner, R.M., Lord Junior, A.E., & Hsuan, Y.H. (1992). Arrhenius modeling to predict geosynthetic degradation. *Geotextiles and Geomembranes*, 11(2), 151-183. https://doi.org/10.1016/0266-1144(92)90042-9.

Lavoie, F.L., Kobelnik, M., Valentin, C.A., Silva Tirelli, É.F., Lopes, M. L., & Silva, J.L. (2022). Evaluation of exhumed HDPE geomembranes used as a liner in Brazilian shrimp farming ponds. *Case Studies in Construction Materials*, 16, e00809. https://doi.org/10.1016/j.cscm.2021.e00809.

Lavoie, F.L., Kobelnik, M., Valentin, C.A., Tirelli, É.F. da S., Lopes, M. L., & da Silva, J.L. (2021). Laboratory study of the ultraviolet radiation effect on an HDPE geomembrane. *Membranes*, 11(6), 390. https://doi.org/10.3390/membranes11060390.

Lavoie, F., Kobelnik, M., Valentin, C., & Silva, J. (2020). Durability of HDPE geomembranes: an overview. *Química Nova*, https://doi.org/10.21577/0100-4042.20170540.

Lin, H., Gong, X., Zeng, Y., & Zhou, C. (2024). Experimental study on the effect of temperature on HDPE geomembrane/geotextile interface shear characteristics. *Geotextiles and Geomembranes*, 52(4), 396-407. https://doi.org/10.1016/j.geotexmem.2023.12.005.

Lodi, P.C. (2003). *Aspectos de degradação de geomembranas poliméricas de polietileno de alta densidade (PEAD) e de poli (cloreto de vinila) (PVC)* [Doctoral thesis]. Escola de Engenharia de São Carlos, Universidade de São Paulo (in Portuguese).

Lopes, H.R., & Silva, J.L. (2024). Shear strength of geomembrane-cohesive soil interfaces. *E3S Web of Conferences*, 569, 01003. https://doi.org/10.1051/e3sconf/202456901003.

Lopes, M.P., & Lopes, M.L. (2010). *A durabilidade dos geossintéticos*. Porto: FEUP Edições.

McWatters, R.S., Rowe, R.K., Di Battista, V., Sfiligoj, B., Wilkins, D., & Spedding, T. (2020). Exhumation and performance of an Antarctic composite barrier system after 4 years exposure. *Canadian Geotechnical Journal*, 57(8), 1130-1152. https://doi.org/10.1139/cgj-2018-0715.

Morsy, M.S., & Rowe, R.K. (2020). Stress crack-resistance of textured geomembranes. In *Proceedings of the Pan American Conference on Geosynthetics* (pp. 1-6), Rio de Janeiro, RJ.

Morsy, M.S. (2019). *Effect of chemical and physical ageing on the longevity of smooth and textured geomembranes in geoenvironmental applications* [Doctoral thesis]. Queen's University, Kingston.

Morsy, M.S., & Rowe, R.K. (2019). Effect of texturing on the longevity of high-density polyethylene (HDPE) geomembranes in municipal solid waste landfills. *Canadian Geotechnical Journal*, 57(1), 61-72. https://doi.org/10.1139/cgj-2019-0047.

Morsy, M.S., & Rowe, R.K. (2017). Effect of texturing on antioxidant depletion rate from HDPE geomembranes. In *Proceedings of the 19th International Conference on Soil Mechanics and Geotechnical Engineering* (pp. 3175-3178), Seoul, South Korea.

Müller, W. (2007). *HDPE geomembranes in geotechnics* (1st ed.). Berlin: Springer. https://doi.org/10.1007/978-3-540-37288-2

Noval, A.M., Blanco, M., Castillo, F., Leiro, A., Mateo, B., Zornberg, J.G., Aguiar, E., Torregrosa, J.B., & Redón, M. (2014). Long-term performance of the HDPE geomembrane at the "San Isidro" reservoir. In *Proceedings of the 10th International Conference on Geosynthetics* (pp. 21-25), Berlin, Germany.

Palmeira, E.M. (2018). *Geossintéticos em geotecnia e meio ambiente*. São Paulo: Oficina de Textos.

Palmeira, E.M. (2025). The Pacheco Silva Lecture 2024 - Geosynthetics and sustainability: solutions to preserve the environment and reduce the effects of climate change. *Soils and Rocks*, 48(2), e202500452. https://doi.org/10.28927/SR.2025.004525.

Pavanello, P., Carrubba, P., & Moraci, N. (2021). The characterisation of geosynthetic interface friction by means of the inclined plane test. *Geotextiles and Geomembranes*, 49(1), 257-275. https://doi.org/10.1016/j.geotexmem.2020.10.027.

Pierozan, R. C., Teixeira, S. H. C., Araújo, G. L. S., & Teixeira, C. A. (2019). Geomembrane as an upstream impermeable blanket of embankment dams: laboratory and numerical study. *Soils and Rocks*, 42(1), 3-19. https://doi.org/10.28927/SR.421003.

Rafter, T., Youngblood, J., & Koerner, G.R. (2018). Case history of a 22-year old geomembrane liner at a domestic waste landfill. In *Proceedings of the 11th International Conference on Geosynthetics (ICG 2018)*, Seoul, South Korea.

Rigo, J.M., & Rollin, A.L. (1990). *Geomembranes-identification and performance testing*. Boca Raton: CRC Press. https://doi.org/10.1201/9781482267501.

Rowe, R.K., & Fan, J. (2024). The application of geosynthetics in tailings storage facilities: a general review. *Mining*, 4(2), 447-468. https://doi.org/10.3390/mining4020026.

Rowe, R.K., Sangam, H.P., & Lake, C.B. (2003). Evaluation of an HDPE geomembrane after 14 years as a leachate lagoon liner. *Canadian Geotechnical Journal*, 40(3), 536-550. https://doi.org/10.1139/t03-019.

Rowe, R.K., & Ewais, A.M.R. (2015). Ageing of exposed geomembranes at locations with different climatological conditions. *Canadian Geotechnical Journal*, 52(3), 326-343. https://doi.org/10.1139/cgj-2014-0131.

Rowe, R.K., & Sangam, H.P. (2002). Durability of HDPE geomembranes. *Geotextiles and Geomembranes*, 20(2), 77-95. https://doi.org/10.1016/S0266-1144(02)00005-5.

Rowe, R.K., & Yu, Y. (2019). Magnitude and significance of tensile strains in geomembrane landfill liners. *Geotextiles and Geomembranes*, 47(3), 439-458. https://doi.org/10.1016/j.geotexmem.2019.01.001.

Rowe, R.K., Abdelaal, F.B., Zafari, M., Morsy, M.S., & Priyanto, D.G. (2020). An approach to high-density polyethylene (HDPE) geomembrane selection for challenging design requirements. *Canadian Geotechnical Journal*, 57(10), 1550-1565. https://doi.org/10.1139/cgj-2019-0572.

Rowe, R.K., Ali, M.M., & Morsy, M.S. (2025). Long-term performance of textured hdpe geomembranes in municipal solid waste landfills. *Canadian Geotechnical Journal*, 62, 1-24. https://doi.org/10.1139/cgj-2024-0024.

Rowe, R. K. (1998). Geosynthetics and the minimization of contaminant migration through barrier systems beneath solid waste. In *Proceeding of the 6th International Conference on Geosynthetics* (Vol. 1), Atlanta, Georgia, USA.

Santos, L.S. (2014). *Estudo da durabilidade de geomembranas utilizadas na impermeabilização de reservatórios das barragens de rejeito de ouro* [Master's dissertation]. Federal University of Minas Gerais (in Portuguese).

Scheirs, J. (2009). *A guide to polymeric geomembranes: a practical approach.* Hoboken: John Wiley & Sons. https://doi.org/10.1002/9780470748213.

Silva, R.A., Abdelaal, F.B., & Rowe, R.K. (2024). A 9-year study of the degradation of a HDPE geomembrane liner used in different high pH mining applications. *Geotextiles and Geomembranes*, 53(1), 230-246. https://doi.org/10.1016/j.geotexmem.2024.09.012.

Soralump, S., Shrestha, A., Jotisankasa, A., Thongthamchart, C., & Isaroran, R. (2021). Use of geosynthetic clay liner as a remedial measure of claystone degradation in Lam Ta Khong hydropower plant. *Geotextiles and Geomembranes*, 49(5), 1211-1228. https://doi.org/10.1016/j.geotexmem.2021.04.001.

Toepfer, G. (2015). *The complete field guide to ensuring quality geosynthetics installations, volume 1: fundamentals & geomembrane.* Integrity Matters.

Urashima, B.M.C., Santos, R., Ferreira, L.D., Inui, T., Urashima, D.C., & Duarte, A.R. (2024). The long-term performance of a high-density polyethylene geomembrane with non-parametric statistic analysis and its contribution to the sustainable development goals. *Applied Sciences*, 14(15), 6821. https://doi.org/10.3390/app14156821.

Valentin, C.A., Silva, J.L., Kobelnik, M., & Ribeiro, C.A. (2018). Thermoanalytical and dynamic mechanical analysis of commercial geomembranes used for fluid retention of leaching in sanitary landfills. *Journal of Thermal Analysis and Calorimetry*, 136(2), 471-481. https://doi.org/10.1007/s10973-018-7690-0.

Valentin, L.A., Valentin, C.A., Kobelnik, M., & Lins da Silva, J. (2022). Chemical characterization of polyethylene geomembranes by chromatography coupled to mass spectrometry using multivariate tools. *Case Studies in Chemical and Environmental Engineering*, 5, 100174. https://doi.org/10.1016/j.cscee.2021.100174.

Xia, X., Pan, Z., Qiu, H., Xie, X., & Guo, K. (2024). Effect of geomembrane liner on landfill stability under long-term loading: interfacial shear test and numerical simulation. *Environmental Science and Pollution Research International*, 31(18), 27345-27355. https://doi.org/10.1007/s11356-024-32953-3.

Xu, G., & Shi, J. (2025). Effect of UV radiation on shear behaviour between geotextile and geomembrane interface. *Geosynthetics International*, 32(3), 440-453. https://doi.org/10.1680/jgein.24.00059.

Xu, G., Shi, J., Liu, Z., Zhang, H., & Gu, Y. (2025). Angle-based residual strength estimation of geotextile/textured geomembrane interface. *Geosynthetics International*, 32(4), 612-623. https://doi.org/10.1680/jgein.24.00115.

Zafari, M., Abdelaal, F.B., & Rowe, R.K. (2023a). Degradation behavior of two multilayered textured white hdpe geomembranes and their smooth edges. *Journal of Geotechnical and Geoenvironmental Engineering*, 149(5), 04023020. https://doi.org/10.1061/JGGEFK.GTENG-11101.

Zafari, M., Abdelaal, F.B., & Rowe, R.K. (2023b). Long-term performance of conductive-backed multilayered hdpe geomembranes. *Geotextiles and Geomembranes*, 51(4), 137-155. https://doi.org/10.1016/j.geotexmem.2023.03.007.

Zafari, M., Rowe, R.K., & Abdelaal, F.B. (2024). Longevity of multilayered textured HDPE geomembranes in low-level waste applications. *Canadian Geotechnical Journal*, 61(4), 684-699. https://doi.org/10.1139/cgj-2023-0039.

Zaharescu, C.A. (2018). *Wear-quantification of textured geomembranes using digital imaging analysis* [Doctoral thesis]. Loughborough University.

Zamara, K.A., Dixon, N., Jones, D.R.V., & Fowmes, G. (2012). Monitoring of a landfill side slope lining system: instrument selection, installation and performance. *Geotextiles and Geomembranes*, 35, 1-13. https://doi.org/10.1016/j.geotexmem.2012.06.003.

Zidan, P., Kemnitz, M., & Ritter, E. (2024). Locating leaks in geomembrane-lined ponds using the electrical leak location method: case histories. *Geotextiles and Geomembranes*, 52(4), 773-777. https://doi.org/10.1016/j.geotexmem.2024.04.003.